

Metabolomic and Transcriptomic Analysis of the Anthocyanin Regulatory Networks in *Malus Domestica* Borkh. Peel with Different Color Patterns

Pengwei Duan

Hebei Academy of Agriculture and Forestry Sciences

Xiaojian Ma

Hebei Academy of Agriculture and Forestry Sciences

Lizhe Qin

Hebei Academy of Agriculture and Forestry Sciences

Jizhuang Du

Hebei Academy of Agriculture and Forestry Sciences

Guoliang Xu

Hebei Academy of Agriculture and Forestry Sciences

Qunzhou Ni

Hebei Academy of Agriculture and Forestry Sciences

Sumiao Yang (✉ 496124424@qq.com)

Hebei Academy of Agriculture and Forestry Sciences

Haiqiang Shi

Hebei Academy of Agriculture and Forestry Sciences

Research Article

Keywords: apple, metabolites, differentially expressed genes, peel coloration, anthocyanin

Posted Date: December 14th, 2021

DOI: <https://doi.org/10.21203/rs.3.rs-1151652/v1>

License:   This work is licensed under a Creative Commons Attribution 4.0 International License. [Read Full License](#)

Abstract

Background: Coloring is an important external quality of 'Fuji' apple (*Malus domestica* Borkh.) and there are two color patterns of apple peels, i.e., stripe and blush. The objectives of this study were to reveal the anthocyanin biosynthesis metabolic pathway in striped and blushed peels of *Malus domestica* using metabolomics and transcriptomics, to identify different anthocyanin metabolites, and to analyze the differentially expressed genes involved in anthocyanin biosynthesis.

Result: The metabolite concentration and gene expression were profiled in the striped and blushed fruit peels of apple harvested at three ripening periods to elucidate the color formation mechanism. At the green fruit period, there were 83 DAMs, including 30 flavonoids, 674 DEGs (521 up-regulated and 153 down-regulated), including 3 MYB related genes (up-regulated, LOC103415449, LOC103421948, LOC103432338) and 2 bHLH genes (up-regulated, LOC103436250, LOC103437863) between striped and blushed apple. At the color turning period, there were 48 DAMs, including 20 flavonoids, 880 DEGs (274 up-regulated and 606 down-regulated), including 3 differentially expressed E2.3.1.133, HCT genes (down-regulated), 2 differentially expressed F3H genes (down-regulated), 1 differentially expressed BZ1 gene (down-regulated) and 2 differentially expressed ANS genes (up-regulated) and 2 up-regulated MYB related genes (LOC103411576, LOC103412495), 5 down-regulated MYB related genes (LOC103400953, LOC103408672, LOC103415404, LOC103420697, LOC103421948), 1 differentially expressed bHLH gene (down-regulated, LOC103400870). At the complete coloring period, there were 95 DAMs, including 34 flavonoids, 2258 DEGs (1159 up- and 1099 down-regulated), including 3 differentially expressed E2.3.1.133, HCT genes (down-regulated), 1 differentially expressed E2.3.1.133, HCT genes (up-regulated), 2 differentially expressed CYP98A genes (up-regulated), 4 differentially expressed CHS genes (up-regulated), 2 differentially expressed E5.5.1.6 genes (up-regulated), 2 differentially expressed CYP75B1 genes (up-regulated), 2 differentially expressed F3R genes (up-regulated), 2 differentially expressed ANS genes (up-regulated), 1 differentially expressed DFR genes (up-regulated), 2 differentially expressed BZ1 genes (up-regulated) and 1 differentially expressed MYB related gene (up-regulated, LOC103401575). There were both 10 kinds of cyanidin in apple peel at color turning period and complete coloring period, Keracyanin and Cyanin were up-regulated at color turning period and Cyanidin-3-O-(6"-O-malonyl)glucoside was up-regulated at complete coloring period.

Conclusions: Our researches provide important information on the anthocyanin metabolites and the candidate genes involved in the anthocyanin biosynthesis pathways of Fuji apple in *M. domestica*.

Background

Apple (*Malus* spp.) is one of the most economically important temperate fruit crops [1]. The quality of the fruit is what people care about most. People in different regions like the color of apple peels differently. Some people like green and some like red. The red varieties are divided into strips and slices. The coloring level of apples is the same as that of other fruits, vegetables, and flowers, and is directly proportional to the type and content of anthocyanins [2–4]. Anthocyanins are water-soluble natural pigments widely found in plants, and are colored aglycones derived from the hydrolysis of anthocyanins [5]. There are more than 200 kinds of anthocyanins known [6], and there are various colors [7]. It plays an important role in helping plants resist pathogens [8], reducing UV damage [9], and preventing pests [10]. At the same time, for humans, it can help us maintain health and fight many diseases [11–12].

Anthocyanins are produced by the secondary metabolism of phenylalanine, and their synthesis and metabolic pathways have been very clearly studied [13]. In some Chinese medicines, forests and other plants, people conduct research on the identification and synthesis of different types of anthocyanins [14–16]. In the direction of horticulture, people's research now focuses more on the effects of transcription factors on the synthesis and transport of anthocyanins [17–18]. The interaction between fruit coloring and other biological processes [19–21].

Some progress has been made in the synthesis and metabolism of anthocyanins in apple research. It has been found that MYB transcription factor [22], NAC transcription factor [23], ethylene [24], B-box protein [25] and so on Both can regulate the synthesis and metabolism of anthocyanins. In addition, genome methylation [26], ectopic expression of F3'H gene [27] and melatonin treatment [28] can also cause differences in anthocyanin expression, but for There are few reports on the difference and mechanism of apple peel coloring of different coloring types. In this paper, two apples with different coloring types, striped red and sliced red, were used for transcription and metabolome determination and analysis to compare, and found the differences in their metabolites. In transcription research, differences were found. These research results may be able to provide some theoretical help to explain

different coloring mechanisms, provide a certain reference for related transcription factors such as anthocyanin transfer and transport, and have great significance for fruit tree cultivation and breeding.

Results

Metabolome Profiling In Apple Peel Over Ripening Stages

Fuji apples changed from yellow-green to red in two weeks after being unbagged during the ripening period. The peel samples were collected at the green fruit period (SF1 and HM1), the color turning period (SF2 and HM2), and the complete coloring period (SF3 and HM3) of the two varieties 'ShiFu' and 'HuiMin' were used for monitoring and changes in the concentration of metabolites related to the coloring process of apple peel (Fig. 1). We profiled the metabolome of the six samples using the widely-targeted metabolomics approach and detected 814 compounds grouped into 36 classes (Table S1). Through principal component analysis of samples (including quality control samples), the PCA results showed that the metabolome separation trend between the groups was obvious, suggesting that there was a difference in metabolome between the sample groups (Fig. 2). The heatmap of metabolites was drawn by R software after unit variance scaling (UV), and hierarchical cluster analysis (HCA) was performed on the accumulation pattern of metabolites among different samples (Fig. 3). We observed that all the biological replicates were grouped together indicating a high-reliability of the generated metabolome data and a clear separation between SF samples and HM samples at three periods, suggesting that the metabolite profiles in these six samples are obviously distinct.

Identification of the differentially accumulated metabolites in different coloring apple fruit peels

The differentially accumulated metabolites (DAM) between pair of samples (SF1 vs HM1, SF2 vs HM2, and SF3 vs HM3) were determined based on the variable importance in projection (VIP) ≥ 1 and fold change ≥ 2 or fold change ≤ 0.5 . As expected, significantly high numbers of metabolites were differentially accumulated between the compared samples, including 83, 48 and 95 DAMs among SF1 vs HM1, SF2 vs HM2, and SF3 vs HM3, respectively (Table S2, S3 and S4). The top enriched KEGG terms between the DAMs detected for all the compared samples were flavone and flavonol biosynthesis, tryptophan metabolism, phenylpropanoid biosynthesis, flavonoid biosynthesis and anthocyanin biosynthesis (Fig. 4A-C). Comparative analysis of the three groups of DAMs among striped and blushed samples resolved to 17 common metabolites (Fig. 4D). Of these, 16 metabolites, including 2 up-accumulated and 14 down-accumulated compounds in the SF samples have constantly conserved the same patterns of differential accumulation (up- or down-) between the two sample types and may contain potential metabolites associated with peel coloration in apple (Table S5). These potential metabolites are from various classes, suggesting that changes in apple peel color may be associated with these factors such as phenolic acids, flavonoids and flavonols. Given the role of flavonoids in plant coloration, we deduce that the DAMs from the flavonoid biosynthesis pathway are likely to be the key metabolites underlying the change in peel coloration of striped and blushed apples. There are 30, 20 and 34 DAMs belonged to flavonoids among SF1 vs HM1, SF2 vs HM2, and SF3 vs HM3, including dihydroflavonol, flavonols, flavonoid, chalcones and anthocyanins.

Anthocyanins are the most important flavonoid colorants in plants (Stintzing & Carle, 2004). A total of 10 anthocyanins were detected in apple peels (Table 1). Over the fruit ripening periods, three anthocyanins were differentially accumulated, including three up-accumulated (Keracyanin, Cyanin and Cyanidin-3-O-(6"-O-malonyl)glucoside) between different color pattern apple (Table 1).

Table 1 Differentially accumulated anthocyanins during the ripening process in apple peel

Metabolite name	Ion abundance						Fold change		
	SF1	HM1	SF2	HM2	SF3	HM3	SF1-vs-HM1	SF2-vs-HM2	SF3-vs-HM3
Cyanidin-3-O-arabinoside	1.31E+05	1.76E+05	1.04E+07	1.61E+07	1.23E+08	1.96E+08	1.34	1.56	1.59
Pelargonidin-3-O-glucoside	-	-	1.44E+05	2.07E+05	1.05E+06	1.04E+06	-	1.44	0.99
Cyanidin-3-O-galactoside	-	-	1.99E+06	2.83E+06	8.58E+06	1.14E+07	-	1.42	1.33
Cyanidin-3-O-glucoside (Kuromanin)	-	-	2.01E+06	2.97E+06	8.62E+06	1.13E+07	-	1.48	1.31
Peonidin-3-O-glucoside	-	-	7.21E+05	1.09E+06	1.28E+06	2.49E+06	-	1.51	1.94
Delphinidin-3-O-glucoside (Mirtillin)	-	-	1.77E+06	2.36E+06	3.98E+06	4.44E+06	-	1.33	1.11
Cyanidin-3-O-(6"-O-malonyl)glucoside	-	-	8.24E+04	1.55E+05	6.07E+05	1.39E+06	-	1.88	2.28(up)
Cyanidin-3-O-(2"-O-xylosyl)galactoside	-	-	4.62E+04	8.79E+04	6.31E+05	8.48E+05	-	1.90	1.34
Cyanidin-3-O-rutinoside (Keracyanin)	-	-	1.23E+05	2.73E+05	4.14E+05	5.92E+05	-	2.22(up)	1.43
Cyanidin-3,5-O-diglucoside (Cyanin)	-	-	7.38E+05	1.50E+06	3.28E+06	4.57E+06	-	2.04(up)	1.40

Transcriptome profiles of apple fruit peels

We further investigated the changes in gene expression profiles among the six peel samples. With three biological replicates, the transcriptome sequencing of the 12 peel samples yielded a total of 117.53 Gb clean data with 93.77% of bases scoring Q30, which showed that all the biological replicates clustered together, indicating the high reliability of our sequencing data (Table S6). Of the total clean reads, 89.28%–90.09% were unique matches with the *Malus domestica* (apple) reference genome (<https://www.ncbi.nlm.nih.gov/genome/browse#!/eukaryo-tes/358/>) (Table S7). We identified 2206 novel genes, 1408 of which were successfully annotated genes, enriching the genomic information available in apple (Table S8). A total of 37,161 unique genes were expressed in apple fruit peel (Table S9).

Principal component analysis (PCA) of the samples based on the number of fragments per kilobase of exon per million fragments mapped (FPKM) values showed that, similar to the metabolome analysis, an obvious separation among the different samples (Fig. 5). Interestingly, we observed that the differences in different periods were greater than the differences between different varieties.

Differentially Expressed Genes In Apple Fruit Peels

Using the criteria $FC > 2$ and $P < 0.05$, 674 DEGs (521 up-regulated and 153 down-regulated) were detected in SF1-vs-HM1, 880 DEGs (274 up- and 606 down-regulated) were detected in SF2-vs-HM2, and 2258 DEGs (1159 up- and 1099 down-regulated) were detected in SF3-vs-HM3, with 60 DEGs being shared among the three comparison groups (Fig. 6). The top enriched KEGG terms contributed by these DEGs were Metabolic pathways and Biosynthesis of secondary metabolites.

Among these DEGs, we found 25 DEGs in the ko00942 (anthocyanin biosynthesis) and ko00941 (flavonoid biosynthesis), including 3 BZ1, 2 ANS, 1 DFR, 4 F3H, 4 CHS, 2 CYP75B1, 2 E5.5.1.6, 2 CYP98A, C3'H and 5 E2.3.1.133, HCT genes. And 11 genes were annotated as MYB-related genes, including LOC103415449, LOC103421948, LOC103432338, LOC103400953, LOC103408672, LOC103415404,

LOC103420697, LOC103421948, LOC103401575, LOC103411576, LOC103412495. Three genes encoding bHLH, LOC103436250, LOC103437863 and LOC103400870. These transcription factors may contribute to anthocyanin metabolite biosynthesis in the peel of apple. Other differently expressed transcription factors were also found in this study, i.e. LOB, NAC, WRKY, GRAS, set, C2H2, AUX/IAA, HB, H3S, HSF, MBF1, NF, TCP, MADS, AP2/ERF, B3, Tify, and OFP.

Modulation Of Anthocyanin Biosynthesis Pathway Genes During Apple Ripening

Previous studies showed that, there were multiple genes and transcription factors involved in structure in the anthocyanin biosynthesis pathway. Combining the results of transcriptomic and metabolomic, 3 MYB related genes (up-regulated, LOC103415449, LOC103421948, LOC103432338) and 2 bHLH genes (up-regulated, LOC103436250, LOC103437863) were found, but with the structure of the anthocyanins related genes and metabolites were not significantly different at the green fruit period.

At the color turning period, compared with blushed apple, there were 3 differentially expressed E2.3.1.133, HCT genes (down-regulated), 2 differentially expressed F3H genes (down-regulated), 1 differentially expressed BZ1 gene (down-regulated) and 2 differentially expressed ANS genes (up-regulated) in striped apple (Fig. 7). On the hand of transcription factors, there were 2 up-regulated MYB related genes (LOC103411576, LOC103412495), 5 down-regulated MYB related genes (LOC103400953, LOC103408672, LOC103415404, LOC103420697, LOC103421948), 1 differentially expressed bHLH gene (down-regulated, LOC103400870). At the same time, Cyanidin-3-O-rutinoside (Keracyanin) and Cyanidin-3,5-O-diglucoside (Cyanin) were up-regulated (Fig. 7).

At the color turning period, compared with blushed apple, there were 3 differentially expressed E2.3.1.133, HCT genes (down-regulated), 1 differentially expressed E2.3.1.133, HCT genes (up-regulated), 2 differentially expressed CYP98A genes (up-regulated), 4 differentially expressed CHS genes (up-regulated), 2 differentially expressed E5.5.1.6 genes (up-regulated), 2 differentially expressed CYP75B1 genes (up-regulated), 2 differentially expressed F3R genes (up-regulated), 2 differentially expressed ANS genes (up-regulated), 1 differentially expressed DFR genes (up-regulated), 2 differentially expressed BZ1 genes (up-regulated) (Fig. 7). And 1 differentially expressed MYB related gene (LOC103401575) and Cyanidin-3-O-(6"-O-malonyl)glucoside was up-regulated (Fig. 7).

Discussion

After the Fuji apples are unpacked, the peel turns from yellow-green to red within 12 days, if the weather is clear and sunny [29]. During this period, anthocyanins accumulate rapidly and the leaf green, carotenoid content decreases in the peel [30]. Some studies have shown that striped red Fuji apples have higher anthocyanin content than slice red [31], which is opposite in this paper. During fruit coloring, hundreds of secondary substances are metabolized in the peel, and these have a great impact on the change of fruit quality [32]. Only some of them, however, are those that have a direct effect on fruit peel coloration, especially the changes in flavonoid content. Flavonoids have a crucial role in human health, and we identified seven groups of flavonoids in ripe apple peels, including Flavonoid, Chalcones, Dihydroflavone, Dihydroflavonol, Flavanols, Isoflavones, Anthocyanins, and Flavonoid carbonoside.

Changes in anthocyanins are responsible for the reddening of the peel [33], but there is no specific anthocyanin type in apples [34–35]. UPLC/electrospray ion trap mass spectrometry is a popular technique in the field of plant metabolite identification and analysis, with the advantages of high sensitivity, high throughput, fast separation and wide coverage. This technique has been widely used for the analysis of metabolites in tomato and asparagus [36, 37]. In this paper, we identified 10 anthocyanin types by extensive targeted metabolomic assays, namely Cyanidin-3-O-arabinoside, Pelargonidin-3-O-glucoside, Cyanidin-3-O-galactoside, Cyanidin-3-O-glucoside (Kuromanin), Peonidin-3-O-glucoside, Delphinidin-3-O-glucoside (Mirtillin), Cyanidin-3-O-(6"-O-malonyl)glucoside, Cyanidin-3-O-(2"-O-xylosyl)galactoside, Cyanidin-3-O-rutinoside (Keracyanin), Cyanidin-3,5-O-diglucoside (Cyanin). Also, before unpacking, there was only one anthocyanin, Cyanidin-3-O-arabinoside, but after starting to color until after complete coloring, there were 10 anthocyanins. Compared with the striped vs blushed, there were 3 anthocyanins with significant differences in content at different periods, namely Cyanidin-3-O-(6"-O-malonyl)glucoside, Cyanidin-3-O-rutinoside (Keracyanin), Cyanidin-3,5-O diglucoside (Cyanin).

Anthocyanin biosynthesis involves three main metabolic pathways, Ko00942 anthocyanin biosynthesis, ko00941 flavonoid metabolism and Ko00940 glutamate metabolism [38]. ANS is one of the four dioxygenases that catalyze anthocyanin formation in

the anthocyanin biosynthetic pathway. Several studies have shown that deletion of ANS and DFR genes in the anthocyanin biosynthetic pathway results in loss of pigmentation [39, 40]. The phenotype of white-fruited snakeberry (Rosaceae) is associated with down-regulation of ANS genes [41]. The repressed expression of ANS genes leads to lack of anthocyanins in *Staphylinia* [42]. In this paper, several differentially expressed genes were identified, including four in CHS, four in F3H, two in ANS, one in DFR, and three in BZ1, and the differential expression of these genes may affect the different coloration types of the pericarp key.

The majority of anthocyanin biosynthesis is regulated by transcription factors at the transcriptional level. So far, transcription factors of Myb, bHLH, WD40, zinc finger, MADs and WRKY proteins have been identified to regulate anthocyanin biosynthesis [43, 44]. Among them, MYB transcription factors play a key role in the regulation of anthocyanin biosynthesis. In particular, MYB75/PAP1 is the main regulator of anthocyanin biosynthesis control in *Arabidopsis* [45]. It has been shown that anthocyanin synthesis in plants is regulated by a protein complex formed by three transcription factors, MYB, bHLH and WD40, which act mainly on the promoters of structural genes of the anthocyanin biosynthetic pathway, and by up-regulating the expression of structural genes, they in turn promote anthocyanin synthesis and accumulation [46–47]. The bHLH transcription factor has been shown to positively regulate anthocyanin biosynthesis in *Arabidopsis* [48]. *mdWRKY11* increases the expression of F3H, FLS, DFR, ANS and UFGT and promotes the accumulation of apple anthocyanins [49]. The *lMADS10* gene regulates anthocyanin biosynthesis to increase the accumulation of anthocyanin pigments in sweet potato [50]. In this paper, 11 differential genes in the MYB family and three differential genes in bHLH were identified in striped red and slice red varieties by transcriptome assays. In addition, other differently expressed transcription factors were also found in this study, i.e. LOB, NAC, WRKY, GRAS, set, C2H2, AUX/IAA, HB, H3S, HSF, MBF1, NF, TCP, MADS, AP2/ERF, B3, Tify, and OFP. which may be related to the different coloration types.

Conclusions

To sum up, we researched and compared the differences between striped and blushed 'Fuji' apple peels by metabolome and transcriptome. The change of flavonoids metabolites, especially anthocyanin biosynthesis and metabolism, underlined the reddening of apple peel. In addition, it was identified that the flavonoids biosynthesis pathways involved in the structure of the mode of gene regulation and transcription factors. These structure genes and its regulation factors (transcription factors) may cause the apple peel anthocyanins in different accumulation and transportation mode and therefore appeared different performance of striped and blushed.

Materials And Methods

Fruit materials

Ten-year old 'ShiFu' and 'HuiMin' *Malus domestica* Borkh. cv. Fuji were used for this study. 'ShiFu' is bred by Shijiazhuang Institute of Pomology, Hebei Academy of Agriculture and Forestry Sciences and 'Huimin' is bred by the Fruit Tree Station of Huimin County, Shandong Province. Both of these varieties have been licensed by the breeding units. 'ShiFu' fruit was covered with red stripes and 'HuiMin' was covered by red color. The trees were grown and maintained at the orchard 'Yuanfang' in Shijiazhuang, China (north latitude 38.259080° east longitude 114.220691° elevation 520m). 'ShiFu' and 'HuiMin' apple fruits were harvested and peeled at green fruit period, color turning period and maturing period and immediately frozen in liquid nitrogen and then stored at -80°C until used.

The peel of apple fruits at the green ripening period (i.e. the peel is fully green) changed from green to red in 12 days after unpacking. Peel samples collected at the green fruit period (1), the color turning period (2) and the complete coloring period (3), were used to monitor changes in metabolite concentration associated with peel coloration process in 'ShiFu' and 'HuiMin' (Fig. 6). We marked the samples of 'ShiFu' as SF1 in green fruit period, as SF2 in color turning period and SF3 in complete coloring period and so did the samples of 'HuiMin' (HM1, HM2 and HM3).

Metabolite extraction

Freeze-dried apple peels were crushed using a mixer mill (MM400, Verder Retsch, Shanghai, China) with a zirconia bead for 1.5 min at a frequency of 30 Hz. Then, 100 mg powder was weighed and extracted overnight at 4 °C with 1.0 mL 70% methanol aqueous solution (V/V = 70%). Following centrifugation at 10,000 g for 10 min, the extracts were absorbed by a CNWBOND Carbon-GCB SPE

cartridge (250 mg, 3 mL; ANPEL, Shanghai, China, www.anpel.com.cn/cnw) and filtered through a 0.22- μ m microfiltration membrane (SCAA-104; ANPEL, Shanghai, China, <http://www.anpel.com.cn/>) before UPLC-MS/MS analysis.

Ultra-performance liquid chromatography (UPLC) Conditions

A UPLC-ESI-MS/MS system (UPLC, Shim-pack UFLC SHIMADZU CBM30A system, Shanghai, China, www.shimadzu.com.cn/) was used to analyze the sample extracts. The UPLC analysis was performed under the following conditions, UPLC: column, Waters (Shanghai, China) ACQUITY UPLC HSS T3 C18 (1.8 μ m, 2.1 mm*100 mm); solvent system, water (0.04% acetic acid); acetonitrile (0.04% acetic acid); gradient program, 95:5 V/V at 0 min, 5:95 V/V at 11.0 min, 5:95 V/V at 12.0 min, 95:5 V/V at 12.1 min, 95:5 V/V at 15.0 min; flow rate, 0.40 mL/min; temperature, 40 °C; injection volume: 2 μ L. The effluent was alternatively connected to an ESI triple quadrupole-linear ion trap (Q TRAP)-MS.

ESI-q trap-MS/MS

Linear ion hydrazine-flight time (LIT) and triple quadrupole (QQQ) scans were conducted on a triple Q TRAP, API 6500 Q TRAP LC/MS/MS system (Applied Biosystems, Shanghai, China) equipped with an ESI turbo ionspray interface, operating in positive ion mode and negative ion mode. The system was controlled by Analyst 1.6 software (AB Sciex, Shanghai, China). The ESI source was set with the following parameters: ion source, turbo spray; source temperature 500 °C; ion spray voltage (IS) 5500 V. The ion source gas I (GSI), gas II (GSII), and curtain gas (CUR) were set at 55.0 psi, 60.0 psi, and 25.0 psi, respectively; the collision gas (CAD) was high. Instrument tuning and mass calibration were performed with 10 and 100 μ mol/L polypropylene glycol solutions in QQQ and LIT modes, respectively. QQQ scans were acquired as multiple reaction monitoring (MRM) experiments with collision gas (nitrogen) set to 5 psi. Declustering potential (DP) collision energy (CE) measurements for individual MRM transitions were completed with further DP and CE optimization. A specific set of MRM transitions was monitored for each period according to the metabolites eluted within the period.

Identification and quantitative analysis of metabolites

Based on the stepwise MIM-EPI (multiple ion monitoring enhanced product ions) to build the commercially available standard Metabolites Database (Metware Biotechnology Co., Ltd. Wuhan, China). The quantitative analysis of metabolites used multiple reaction monitoring [51, 52]. Unsupervised PCA (principal component analysis), HCA (hierarchical cluster analysis), and OPLS-DA (partial least-squares discriminant analysis) were performed by the statistics function prcomp within R (www.r-project.org). Significantly different metabolites between groups were determined by VIP ≥ 1 and fold change ≥ 2 or fold change ≤ 0.5 .

RNA extraction and Illumina sequencing

Total RNA was extracted from frozen apple peels using the RNeasy Pure Plant Kit (Qiagen Biotech, Beijing, China). RNA degradation and contamination were monitored on 1.2% agarose gels. The purified RNA concentrations were quantified using a NanoDrop™ 2000 spectrophotometer (Thermo Scientific, Shanghai, China). The quality of the total RNA was examined using an Agilent 2100 Bioanalyzer (Agilent Technologies, Santa Clara, CA, USA). Poly (A) mRNA was enriched from the total RNA using Oligo (dT) magnetic beads. Poly (A) mRNA was subsequently fragmented by an RNA fragmentation kit (Ambion, Austin, TX, USA). The fragmented RNA was transcribed into first-strand cDNA using reverse transcriptase and random hexamer primers. Second-strand cDNA was synthesized using DNA polymerase I and RNase H (Invitrogen, Carlsbad, CA, USA). After end repair and the addition of a poly (A) tail, suitable length fragments were isolated and connected to the sequencing adaptors. The fragments were sequenced on an Illumina HiSeq™ 2500 platform.

RNA sequencing (RNA-seq) data analysis and annotation

To acquire high-quality reads, the raw reads in fastq format were processed through in-house Perl scripts. Clean reads were obtained from raw data by removing adaptor sequences, low-quality reads, and reads containing ployN. All downstream analyses were based on clean, high-quality data. Gene function was annotated using the following: the Kyoto Encyclopedia of Gene and Genome (KEGG) pathway database, the NCBI non-redundant (Nr) database, the Swiss-Prot protein database, the euKaryotic Clusters of Orthologous Groups (KOG) database, the Gene Ontology (GO) database, and the Pfam database.

The levels of gene expression were estimated by RSEM (version 1.2.26) [53]. Analysis of the differentially expressed genes of the two groups was performed with the DESeq R package (1.10.1). DESeq provides statistical routines for determining differentially expressed genes using a model based on the negative binomial distribution. The results of all statistical tests were corrected by multiple tests using the Benjamini and Hochberg false discovery rate. Genes were determined to be significantly differentially expressed at an adjusted P-value of < 0.05 according to DESeq. GO enrichment analysis of the differentially expressed genes was implemented by the topGO R package based on the Kolmogorov-Smirnov test. Pathway analysis elucidated significant pathways of differentially expressed genes according to the KEGG database (<http://www.genome.jp/kegg/>) [54]. We tested the statistical enrichment of differentially expressed genes in KEGG pathways using KOBAS software [55].

Statistical analysis

Statistical analysis was performed using Excel 2010 software (Microsoft Office, USA). Data are presented as means \pm standard deviations (SD). The levels of statistical significance were analyzed by the least significant difference ($p < 0.05$).

Abbreviations

DFR
Dihydroflavonol 4-reductase
ANS
Anthocyanidin synthase
UFGT
Anthocyanidin 3-O-glucosyltransferase
CHS
Chalcone synthase
CHI
Chalcone isomerase
F3H
Flavonone 3-hydroxylase
F3'H
Flavonoid 3'-monooxygenase
F3'5'H
Flavonoid 3',5'-hydroxylase
bHLH
Basic helix-loop-helix
DEGs
Differentially expressed genes
PCA
Principal component analysis
HCA
Hierarchical cluster analysis
OPLS-DA
Partial least-squares discriminant analysis
KEGG
Kyoto Encyclopedia of Gene and Genome
KOG
EuKaryotic Clusters of Orthologous Groups
GO
Gene Ontology.

Declarations

Acknowledgements

We appreciate Wuhan MetWare Biotechnology Co., Ltd. (www.metware.cn) for providing metabolomics services.

Authors' contributions

SM and HQ conceived and designed the experiments. XJ, GL, and LZ performed the experiments. QZ and JZ analyzed the data. PW wrote the paper. The authors read and approved the final version of the paper.

Funding

This work was supported by the Technical System of Fruit Industry in Hebei Province (HBCT2018100201), Key Research and Development Project of Hebei Province (19226818D), and Innovative Engineering Project of Hebei Academy of Agriculture and Forestry Sciences (2019-3-6-1). The funders had no role in the design of the study, data collection, analysis and interpretation, decision to publish, or preparation of the manuscript.

Availability of data and materials

The link of *Malus domestica* (apple) reference genome database is open (<https://www.ncbi.nlm.nih.gov/genome/browse#!/eukaryotes/358/>). Other relevant supporting data sets are included in the article and its supplemental files.

Ethics approval and consent to participate

Not applicable.

Consent for publication

Not applicable.

Competing interests

The authors declare that they have no conflict of interest.

References

1. Wang MR, Chen L, Teixeira da Silva JA, Volk GM, Wang QC. Cryobiotechnology of apple (*Malus* spp.): development, progress and future prospects. *Plant Cell Rep.* 2018;37(5):689-709.
2. Sun L, Li S, Tang X, Fan X, Zhang Y, Jiang J, Liu J, Liu C. Transcriptome analysis reveal the putative genes involved in light-induced anthocyanin accumulation in grape 'Red Globe' (*V. vinifera* L.). *Gene.* 2020; 728:144284.
3. Wang H, Sun S, Zhou Z, Qiu Z, Cui X. Rapid analysis of anthocyanin and its structural modifications in fresh tomato fruit. *Food Chem.* 2020; 333:127439.
4. Nuraini L, Ando Y, Kawai K, Tatsuzawa F, Tanaka K, Ochiai M, Suzuki K, Aragonés V, Daròs JA, Nakatsuka T. Anthocyanin regulatory and structural genes associated with violet flower color of *Matthiola incana*. *Planta.* 2020;251(3):61.
6. Jaakola L. New insights into the regulation of anthocyanin biosynthesis in fruits. *Trends Plant Sci.* 2013;18(9):477-83.
7. Silva S, Costa EM, Calhau C, Morais RM, Pintado ME. Anthocyanin extraction from plant tissues: A review. *Crit Rev Food Sci Nutr.* 2017;57(14):3072-3083.
8. Sharma RR, Pal RK, Sagar VR, Parmanick KK, Rana MR, Gupta VK, et al. Impact of pre-harvest fruit-bagging with different coloured bags on peel colour and the incidence of insect pests, disease and storage disorders in 'Royal Delicious' apple. *J Hortic Sci Biotechnol.* 2014;89(6):603–18.
9. Sharma A, Shahzad B, Rehman A, Bhardwaj R, Landi M, Zheng B. Response of Phenylpropanoid Pathway and the Role of Polyphenols in Plants under Abiotic Stress. *Molecules.* 2019;24(13):2452.

10. Bentley WJ, Viveros M. Brown-bagging 'granny Smith' apples on trees stops codling moth damage. *Calif Agric.* 1992;46(4):30–2.
11. Lila MA, Burton-Freeman B, Grace M, Kalt W. Unraveling Anthocyanin Bioavailability for Human Health. *Annu Rev Food Sci Technol.* 2016;7:375-93.
12. Lee YM, Yoon Y, Yoon H, Park HM, Song S, Yeum KJ. Dietary Anthocyanins against Obesity and Inflammation. *Nutrients.* 2017;9(10):1089.
13. Shi MZ, Xie DY. Biosynthesis and metabolic engineering of anthocyanins in *Arabidopsis thaliana*. *Recent Pat Biotechnol.* 2014;8(1):47-60.
14. Jiang T, Zhang M, Wen C, Xie X, Tian W, Wen S, Lu R, Liu L. Integrated metabolomic and transcriptomic analysis of the anthocyanin regulatory networks in *Salvia miltiorrhiza* Bge. flowers. *BMC Plant Biol.* 2020;20(1):349.
15. Wang L, Pan D, Liang M, Abubakar YS, Li J, Lin J, Chen S, Chen W. Regulation of Anthocyanin Biosynthesis in Purple Leaves of Zijuan Tea (*Camellia sinensis* var. *kitamura*). *Int J Mol Sci.* 2017;18(4):833.
16. Zhang Y, Chen G, Dong T, Pan Y, Zhao Z, Tian S, Hu Z. Anthocyanin accumulation and transcriptional regulation of anthocyanin biosynthesis in purple bok choy (*Brassica rapa* var. *chinensis*). *J Agric Food Chem.* 2014;62(51):12366-76.
17. Xi X, Zha Q, Jiang A, Tian Y. Impact of cluster thinning on transcriptional regulation of anthocyanin biosynthesis-related genes in 'Summer Black' grapes. *Plant Physiol Biochem.* 2016;104:180-7.
18. Cao K, Ding T, Mao D, Zhu G, Fang W, Chen C, Wang X, Wang L. Transcriptome analysis reveals novel genes involved in anthocyanin biosynthesis in the flesh of peach. *Plant Physiol Biochem.* 2018;123:94-102.
19. Das PK, Geul B, Choi SB, Yoo SD, Park YI. Photosynthesis-dependent anthocyanin pigmentation in *Arabidopsis*. *Plant Signal Behav.* 2011;6(1):23-5.
20. Yong Y, Zhang Y, Lyu Y. A MYB-Related Transcription Factor from *Lilium lancifolium* L. (LIMYB3) Is Involved in Anthocyanin Biosynthesis Pathway and Enhances Multiple Abiotic Stress Tolerance in *Arabidopsis thaliana*. *Int J Mol Sci.* 2019;20(13):3195.
21. Zhou Y, Yuan C, Ruan S, Zhang Z, Meng J, Xi Z. Exogenous 24-Epibrassinolide Interacts with Light to Regulate Anthocyanin and Proanthocyanidin Biosynthesis in Cabernet Sauvignon (*Vitis vinifera* L.). *Molecules.* 2018;23(1):93.
22. An JP, Wang XF, Zhang XW, Xu HF, Bi SQ, You CX, Hao YJ. An apple MYB transcription factor regulates cold tolerance and anthocyanin accumulation and undergoes MIEL1-mediated degradation. *Plant Biotechnol J.* 2020;18(2):337-353.
23. Sun Q, Jiang S, Zhang T, Xu H, Fang H, Zhang J, Su M, Wang Y, Zhang Z, Wang N, Chen X. Apple NAC transcription factor MdNAC52 regulates biosynthesis of anthocyanin and proanthocyanidin through MdMYB9 and MdMYB11. *Plant Sci.* 2019;289:110286.
24. Zhang J, Xu H, Wang N, Jiang S, Fang H, Zhang Z, Yang G, Wang Y, Su M, Xu L, Chen X. The ethylene response factor MdERF1B regulates anthocyanin and proanthocyanidin biosynthesis in apple. *Plant Mol Biol.* 2018;98(3):205-218.
25. Bai S, Saito T, Honda C, Hatsuyama Y, Ito A, Moriguchi T. An apple B-box protein, MdCOL11, is involved in UV-B and temperature-induced anthocyanin biosynthesis. *Planta.* 2014 ;240(5):1051-62.
26. Li WF, Ning GX, Mao J, Guo ZG, Zhou Q, Chen BH. Whole-genome DNA methylation patterns and complex associations with gene expression associated with anthocyanin biosynthesis in apple fruit skin. *Planta.* 2019;250(6):1833-1847.
27. Han Y, Vimolmangkang S, Soria-Guerra RE, Rosales-Mendoza S, Zheng D, Lygin AV, Korban SS. Ectopic expression of apple F3'H genes contributes to anthocyanin accumulation in the *Arabidopsis* tt7 mutant grown under nitrogen stress. *Plant Physiol.* 2010;153(2):806-20.

28. Chen L, Tian J, Wang S, Song T, Zhang J, Yao Y. Application of melatonin promotes anthocyanin accumulation in crabapple leaves. *Plant Physiol Biochem.* 2019;142:332-341.
29. Lee S. K., Kim K, Bae R, and Kim T. Anatomical observations of anthocyanin rich cells in apple skins, *Hort Science*, 2006;41: 733-736
30. Wang S.M., Gao H.J., and Zhang X.B. Effects of bagging on pigment, sugar and acid development in 'Red Fuji' Apple fruits, *Acta Horticulturae Sinica*, 2002;3: 263-265
31. Chi X, Wang X, Liu X, Jiang Z, Sylwia Keller-Przybylkowicz, Song L, Du X. The Variation of Color-associated Factors of Fuji Apple with Different Color Patterns after Bag Removal. *Molecular Plant Breeding.* 2021,19(05):1649-1656.
32. Zhang Q, Wang L, Liu Z, Zhao Z, Zhao J, Wang Z, Zhou G, Liu P, Liu M. Transcriptome and metabolome profiling unveil the mechanisms of *Ziziphus jujuba* Mill. peel coloration. *Food Chem.* 2020;312:125903.
33. Ma C, Liang B, Chang B, Yan J, Liu L, Wang Y, Yang Y, Zhao Z. Transcriptome profiling of anthocyanin biosynthesis in the peel of 'Granny Smith' apples (*Malus domestica*) after bag removal. *BMC Genomics.* 2019;20(1):353.
34. Chen W, Zhang M, Zhang G, Li P, Ma F. Differential Regulation of Anthocyanin Synthesis in Apple Peel under Different Sunlight Intensities. *Int J Mol Sci.* 2019;20(23):6060.
35. Zhang X, Huo H, Sun X, Zhu J, Dai H, Zhang Y. Nanocrystallization of Anthocyanin Extract from Red-Fleshed Apple 'QN-5' Improved Its Antioxidant Effect through Enhanced Stability and Activity under Stressful Conditions. *Molecules.* 2019;24(7):1421.
36. Zhu G, Wang S, Huang Z, Zhang S, Lia Q, Zhang C, et al. Rewiring of the fruit metabolome in tomato breeding. *Cell.* 2018;172:249–61.
37. Paolo B, Saverio O, Mirko M, Matteo B, Lara G, Azeddine SA. Gene expression and metabolite accumulation during strawberry (*Fragaria x ananassa*) fruit development and ripening. *Planta.* 2018;248(5):1143–57
38. Meng G, Clausen SK, Rasmussen SK. Transcriptome Analysis Reveals Candidate Genes Related to Anthocyanin Biosynthesis in Different Carrot Genotypes and Tissues. *Plants (Basel).* 2020;9(3):344.
39. Bogs J, Jaffe FW, Takos AM, Walker AR, Robinson SP. The grapevine transcription factor VvMYBPA1 regulates proanthocyanidin synthesis during fruit development. *Plant Physiol.* 2007;143:1347–61.
40. Clark ST, Verwoerd WS. A systems approach to identifying correlated gene targets for the loss of colour pigmentation in plants. *BMC Bioinformatics.* 2011;12:343.
41. Debes MA, Arias ME, Grellet-Bournonville CF, Wulff AF, Martínez Zamora MG, Castagnaro AP, et al. White-fruited *Duchesnea Indica* (Rosaceae) is impaired in ANS gene expression. *Am J Bot.* 2011;98(12):2077–83.
42. Shimada S, Inoue YT, Sakuta M. Anthocyanidin synthase in nonanthocyanin-producing Caryophyllales species. *Plant J.* 2005;44(6):950–9.
43. Terrier N, Torregrosa L, Ageorges A, Vialet S, Verries C, Cheynier V, et al. Ectopic expression of VvMybPA2 promotes proanthocyanidin biosynthesis in grapevine and suggests additional targets in the pathway. *Plant Physiol.* 2008;149(2):1028–41.
44. Lloyd A, Brockman A, Aguirre L, Campbell A, Bean A, Cantero A, et al. Advances in the MYB–bHLH–WD repeat (MBW) pigment regulatory model: addition of a WRKY factor and co-option of an anthocyanin MYB for betalain regulation. *Plant Cell Physiol.* 2017;58(9):1431–41.
45. Solfanelli C, Poggi C, Loreti E, Alpi A, Perata P. Sucrose-specific induction of the anthocyanin biosynthetic pathway in *Arabidopsis*. *Plant Physiol.* 2006;140:637–46.

46. Chen L, Hu B, Qin Y, Hu G, Zhao J. Advance of the negative regulation of anthocyanin biosynthesis by MYB transcription factors. *Plant Physiol Biochem.* 2019;136:178-187.
47. Hichri I, Barrieu F, Bogs J, Kappel C, Delrot S, Lauvergeat V. Recent advances in the transcriptional regulation of the flavonoid biosynthetic pathway. *J Exp Bot.* 2011;62(8):2465–83.
48. Shi MZ, Xie DY. Biosynthesis and metabolic engineering of anthocyanins in *Arabidopsis thaliana*. *Recent Pat Biotechnol.* 2014;8:47–60.
49. Wang N, Liu W, Zhang T, Jiang S, Xu H, Wang Y, et al. Transcriptomic analysis of red-fleshed apples reveals the novel role of MdWRKY11 in flavonoid and anthocyanin biosynthesis. *J Agric Food Chem.* 2018;6(27):7076–86.
50. Lalusin A, Ocampo E, Fujimura T. *Arabidopsis thaliana* plants overexpressing the IbMADS10 gene from sweetpotato accumulates high level of anthocyanin. *Philipp J Crop Sci.* 2011;36(2):30–6.
51. Chen W, Gong L, Guo Z, Wang W, Zhang H, Liu X, et al. A novel integrated method for large-scale detection, identification, and quantification of widely targeted metabolites: application in the study of rice metabolomics. *Mol Plant.* 2013;6:1769–80.
52. Wang ZR, Cui YY, Vainstein A, Chen SW, Ma HQ. Regulation of fig (*Ficus carica* L.) fruit color: Metabolomic and transcriptomic analyses of the flavonoid biosynthetic pathway. *Front Plant Sci.* 2017. <https://doi.org/10.3389/fpls.2017.01990>.
53. Li JJ, Jiang CR, Brown JB, Huang H, Bickel PJ. Sparse linear modeling of next-generation mRNA sequencing (RNA-Seq) data for isoform discovery and abundance estimation. *P Natl Acad Sci USA.* 2011;108:19867–72.
54. Kanehisa M, Araki M, Goto S, Hattori M, Hirakawa M, Itoh M, et al. KEGG for linking genomes to life and the environment. *Nucleic Acids Res.* 2007;36:480–4.
55. Mao X, Cai T, Olyarchuk JG, Wei L. Automated genome annotation and pathway identification using the KEGG Orthology (KO) as a controlled vocabulary. *Bioinformatics.* 2005;21:3787–93.

Figures

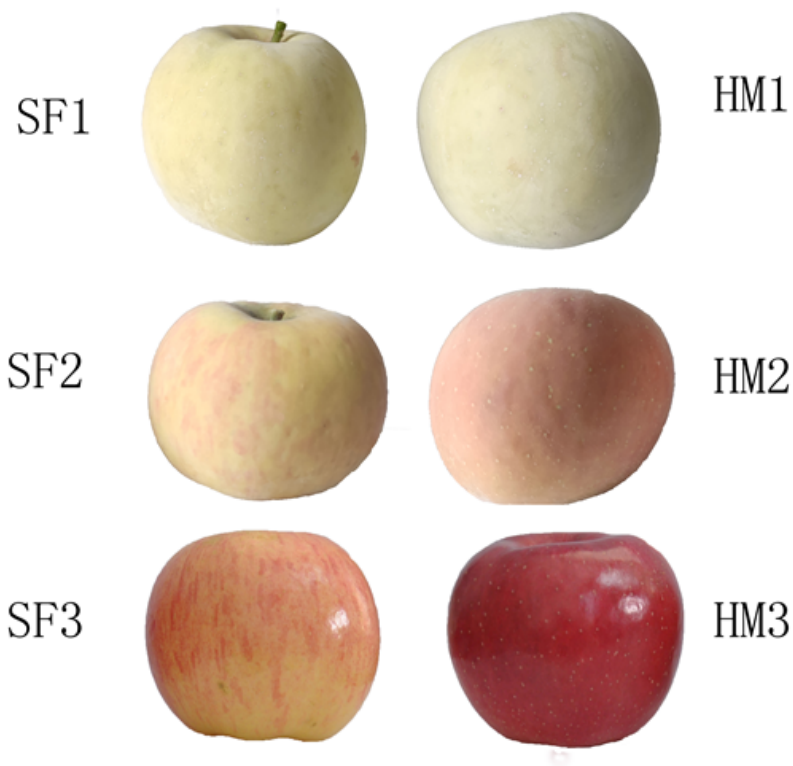


Figure 1

The phenotypes of the apple during different ripening periods

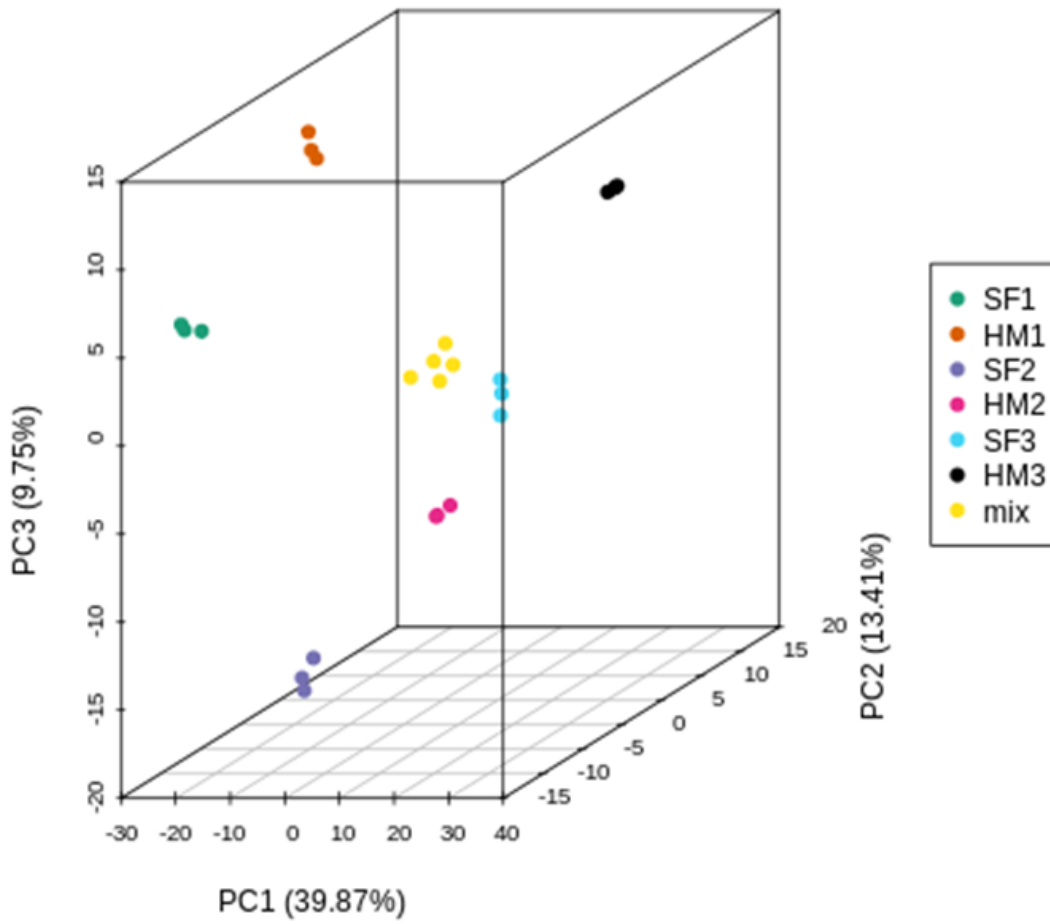


Figure 2

Principal component analysis of the six peel samples based on the metabolome

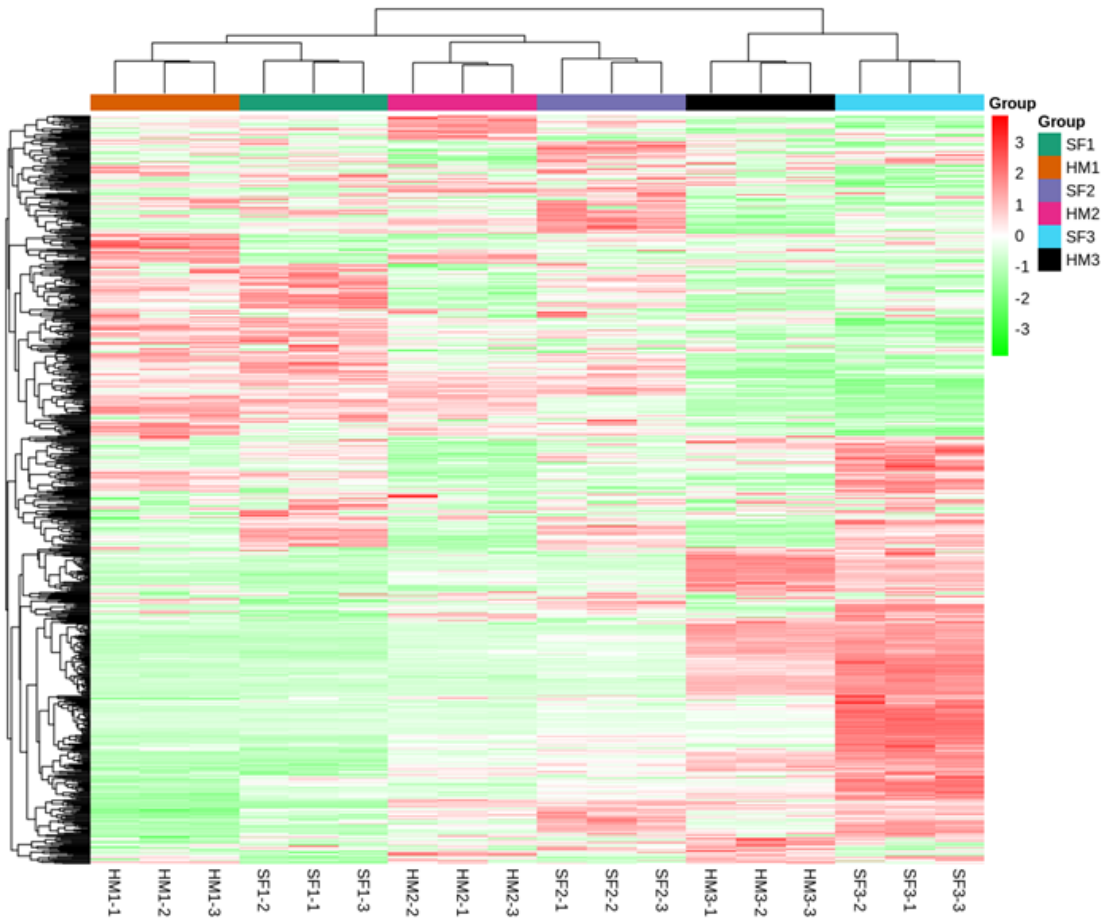


Figure 3

The hierarchical heatmap clustering analysis of the apple peels

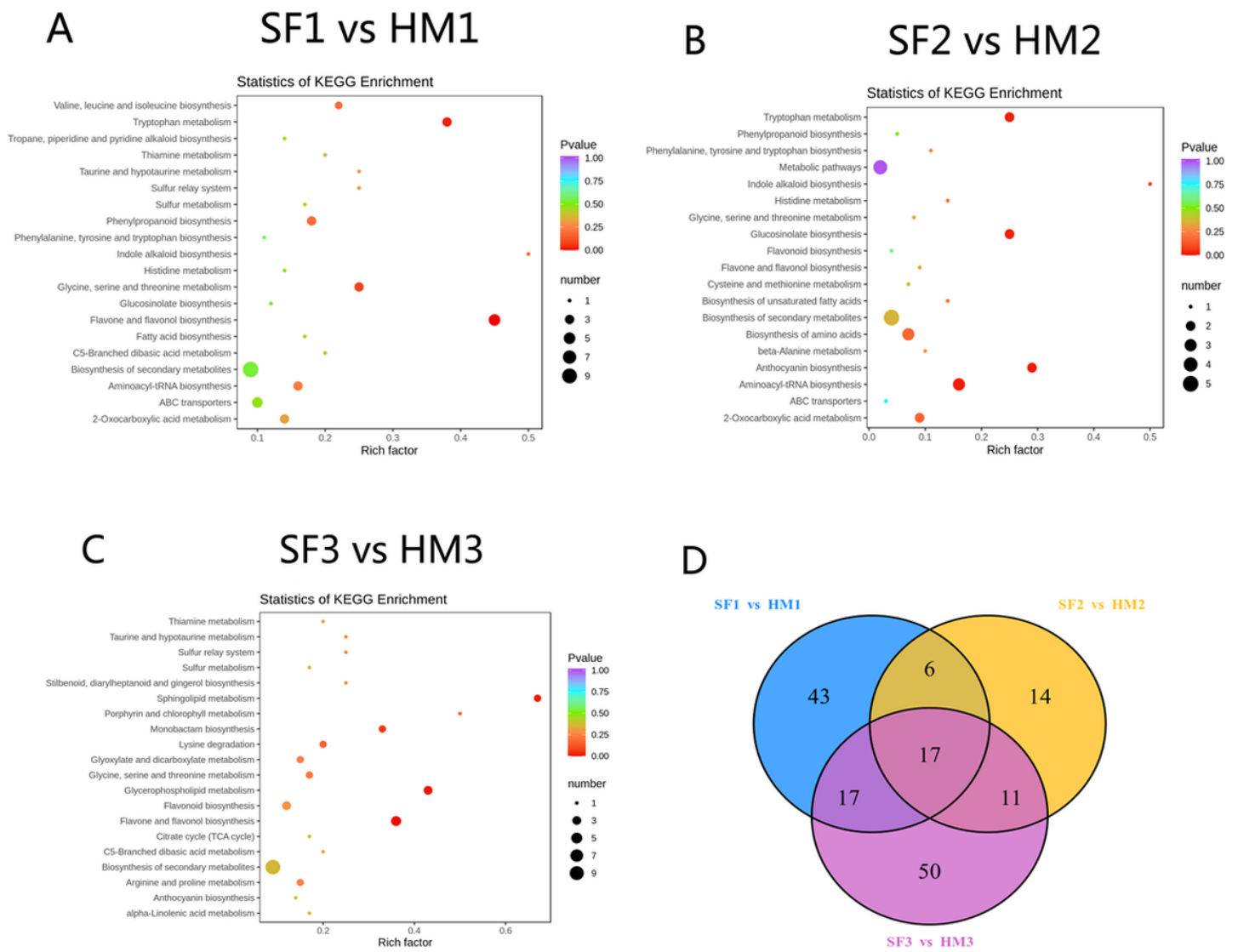


Figure 4

Identification and functional characterization of the differentially accumulated metabolites (DAMs) between SF and HM apple peel samples. KEGG enrichment analysis of the DAMs between (A) SF1 vs HM1, (B) SF2 vs HM2 and (C) SF1 vs HM1, (D) Venn diagram depicting the shared and specific metabolites between the six compared groups of peel samples.

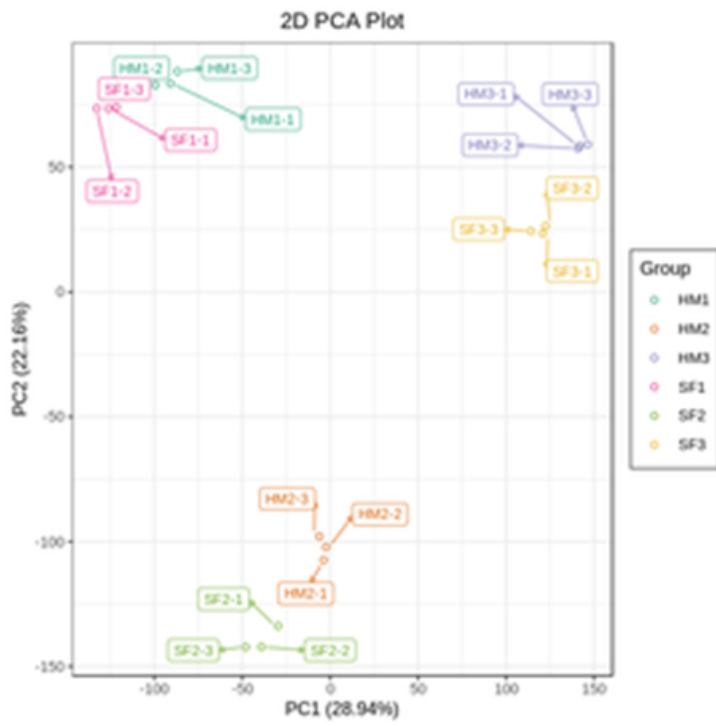


Figure 5

Principal component analysis of the six peel samples based on the gene expression profiles

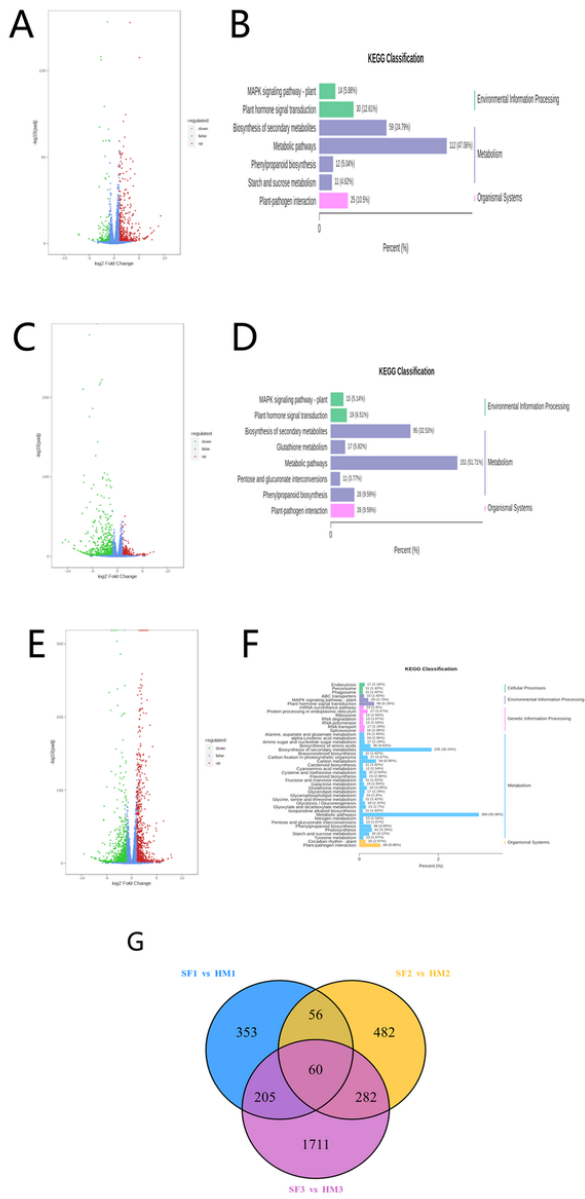


Figure 6

Differential expressed genes (DEG) in peel of apple during ripening. (A) Volcano plots

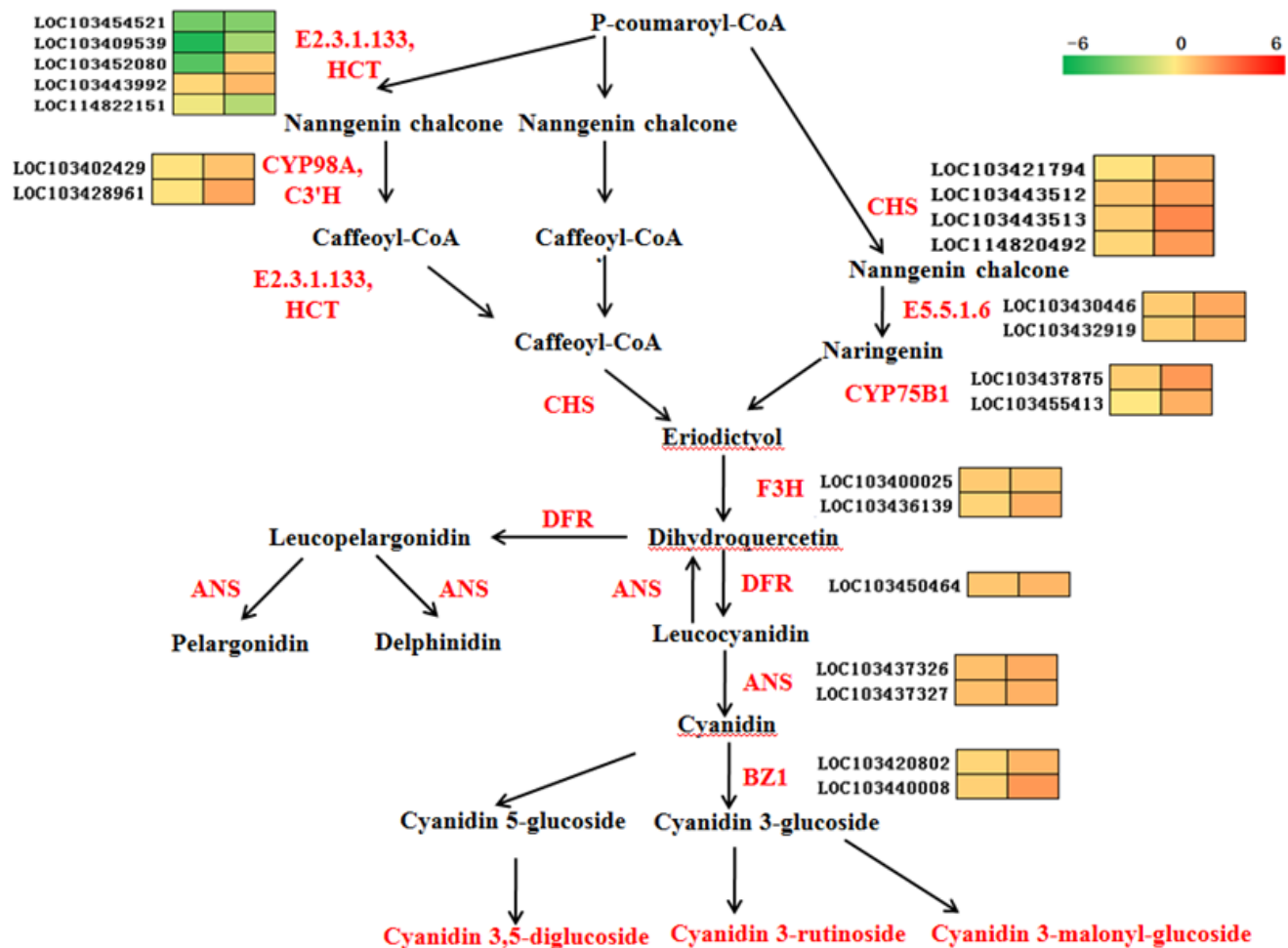


Figure 7

Biosynthetic pathway of anthocyanin in SF and HM

Supplementary Files

This is a list of supplementary files associated with this preprint. Click to download.

- [TableS1.Allofthemetabolicdata..xls](#)
- [TableS2.DifferentmetabolitesinSF1vs.HM1..xls](#)
- [TableS3.DifferentmetabolitesinSF2vs.HM2..xls](#)
- [TableS4.DifferentmetabolitesinSF3vs.HM3..xls](#)
- [TableS5.ThedataofVennpictureinmetabolites..xls](#)
- [TableS6.TheQ30dataoftranscriptome..xls](#)
- [TableS7.Theuniquematchesgene.xls](#)
- [TableS8.Thedataofnovelgenes..xls](#)
- [TableS9.Thedataofuniquegenes..xls](#)
- [TableS10.DifferentiallyexpressedgenesofTFinSF1vs.HM1..xls](#)
- [TableS11.DifferentiallyexpressedgenesofTFinSF2vs.HM2..xls](#)
- [TableS12.DifferentiallyexpressedgenesofTFinSF3vs.HM3..xls](#)